New mechanism for press-fit processes: preliminary analysis

Lorenzo Fiorineschi, Luca Pugi and Federico Rotini
Department of Industrial Engineering, University of Florence, Florence, Italy

Abstract

Purpose – The purpose of this paper is to present an alternative solution for press-fit technology processes, which could improve the precision of the positioning movements and the stiffness of the structural elements.

Design/methodology/approach – A concept is presented and the related kinematics is described. Then, preliminary embodiment evaluations have been performed in terms of kinematics, force control and load distribution on the main structural elements.

Findings – Thanks to the additional leg, the proposed solution allows a preload that is capable of compensating the backlash of joints. The particular structure with four extendible legs and eight cardan joints ensures the parallelism between the ground and the plate holding the end effector, without any need of additional controls. However, it implies that the legs are not subjected to pure tension–compression stresses.

Research limitations/implications – This work is focused on the conceptual phase of the design process, with only preliminary embodiment analysis that paves the way for subsequent and more detailed design steps. Especially concerning the actual stiffness of the system, comprehensive evaluations could be performed only after the identification of the particular parts/devices used to implement the main functional elements.

Originality/value – To the best of the authors' knowledge, this is the first research work that comprehensively describes and analyzes the considered kinematics, within a real industrial application context.

Keywords Parallel mechanism, Conceptual design, Mechatronics, Press-fit technology, Three DOFs

Paper type Case study

1. Introduction

The press-fit technology (Chen, 2008) constitutes an extension of the conventional through hole technology (THT), where the fixed electronic component is provided with a pin made by elasto-plastic material. The press-fit technology is largely used for electronic boards manufacturing processes and allows high production rates. In this process, the pin is inserted in the electronic board by means of a specific pressing element, and the friction-interference between the pin and the board's hole ensures the stability of the electronic component (Figure 1). This manufacturing approach is particularly suited for power electronics of vehicular applications as the obtained fixture is claimed to be more resilient respect to classic soldered junctions. This is a very interesting feature especially for power equipment subjected to high level of vibrations or to mechanical shock, in which resilience of the connection should make the difference in terms of reliability.

Usually, the machines used to perform press-fit assembly of large power electronic components are typically based on a Cartesian layout (Peruzzi *et al.*, 2021) such as the one shown in Figure 2. Generally, relatively robust structure is needed to hold the end effector, which is required to exert relatively high vertical forces (600–700 N for the example of Figure 2), with the required accuracy of position.

Accordingly, the main problem of this kind of systems resides in the overall stiffness of the Cartesian structure. Indeed, because of the active force that can be relatively far from supports, the X and Z elements (Figure 2) are prevalently subjected to non-negligible bending moments.

The aim of this work is to propose an alternative solution, capable to comply with the following specifications:

- Identification of an alternative kinematics allowing a more efficient distribution of the active load.
- A precise control of vertical forces to reduce size and complexity of end effector.
- A design that should exploit recent technology trends related to industry and robotics 4.0 (Haidegger *et al.*, 2019).

The originality of this work is mainly related to the analysis of the proposed solution, which is rather unusual if compared with classical devices that are commonly proposed in literature for similar applications [e.g. delta manipulators (Botello-Aceves *et al.*, 2018) or Cartesian parallel manipulators such as the multipteron ones (Gosselin *et al.*, 2007)].

The current issue and full text archive of this journal is available on Emerald Insight at: **https://www.emerald.com/insight/1708-5284.htm**

World Journal of Engineering
Emerald Publishing Limited [ISSN 1708-5284]
[DOI 10.1108/WJE-03-2021-0120]

© Lorenzo Fiorineschi, Luca Pugi and Federico Rotini. Published by Emerald Publishing Limited. This article is published under the Creative Commons Attribution (CC BY 4.0) licence. Anyone may reproduce, distribute, translate and create derivative works of this article (for both commercial and non-commercial purposes), subject to full attribution to the original publication and authors. The full terms of this licence may be seen at http://creativecommons.org/licences/by/4.0/legalcode

Received 1 March 2021
Revised 26 April 2021
Accepted 24 May 2021

Figure 1 Figure 1 Press-fit tecnology using a friction/elastic THT

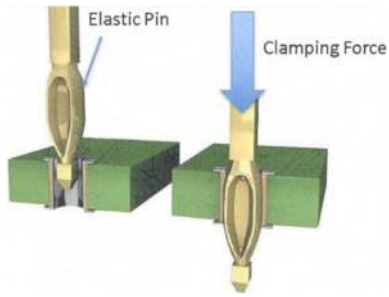

Figure 2 Example of a Cartesian machine for press-fit assembly of power electronic components (Peruzzi *et al.*, 2021)

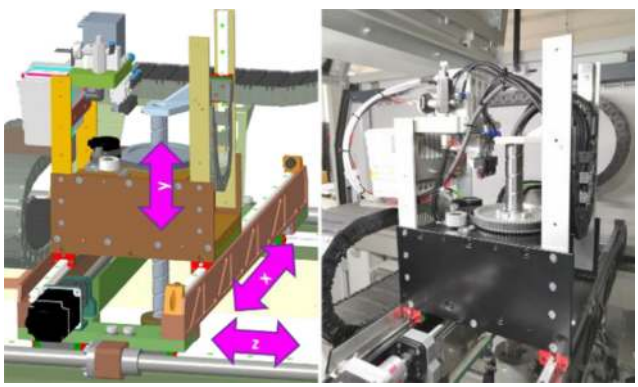

Proposed manipulator differs from recent solutions (Achilli *et al.*, 2020) concerning precise manipulation with modular embedded constraints.

The contents are distributed as follows. Section 2 describes the methodological approach used to conceive and investigate the proposed solution. Section 3 illustrates the results from the kinematic analysis, while the results from load distribution analysis are reported in Section 4. Discussions and possible hints for the implementation of mechanical components are reported in Section 5. In the same section, the limits of the work and the impact expected for both academia and industry are described.

2. Design approach

A variety of models and methods have been proposed in the literature, respectively, describing the design process and guiding the designers in performing it (Wynn and Clarkson, 2017). Among them, the so-called German systematic design approach is one of the most acknowledged in literature (Le Masson and Weil, 2012; Beitz *et al.*, 1987). The particular version described by G. Pahl and W. Beitz (Pahl *et al.*, 2007) represents the most diffused versions of the recalled approach. It is constituted by four key phases, i.e. the clarification of the design task, the conceptual design, the embodiment design and the detail design (Pahl *et al.*, 2007).

The task clarification phase aims at identifying the objectives of the design activity, with an expected outcome constituted by a structured list of engineering requirements. The latter constitutes the starting point for the conceptual design phase, which aims at identifying solutions capable to implement the main functions expected for the system, as well as first sketches of potential solution alternatives. At the end of this step, the fundamentals for the subsequent design phases are defined, and this is why it is acknowledged to be a crucial step in the design process, influencing the 60%–80% of the design costs (Akay *et al.*, 2011; Bernard *et al.*, 2014).

Then, the concept details are gradually developed in the embodiment and detail design phases, by facing incrementally detailed issues characterizing the specific solutions selected in the conceptual design phase. In particular, in the embodiment design phase, early virtual and/or physical prototypes can be realized for the product or part of it, to gather important information about the feasibility of the adopted solutions.

Figure 3 schematically represents the main phases of the systematic design process followed in this work. However, it is worth to notice that even if not represented in Figure 3, the overall design process is highly iterative, and then design iterations are normally expected among the different design phases (Pahl *et al.*, 2007).

This work focuses the attention on the conceptual design phase, because it aims at proposing an alternative solution for press-fit processes, without particular limits in terms of similitude with current machines. Accordingly, such a kind of task allows investigating quite different principles to develop the underpinning kinematic.

The task clarification process was quite simple in this case, because besides the geometrical limits imposed by the boards and the force needed to press the pins, no constraints have been provided for this preliminary investigation activity.

Therefore, after the identification of the preferred solution, the conceptual design focused on preliminary schematizations and kinematic evaluations. Then, preliminary embodiment models are used here only to gather information about load distributions, which are fundamental for performing the succeeding design activities (e.g. selecting actuators, guides and designing joints).

3. Proposed concept

To increase the stiffness of the device, the authors of this paper took inspiration from classical construction theory and practice that suggests using tension/compression only elements. By thinking about orientable telescopic elements that could move

Figure 3 Steps of the systematic design process considered in this work

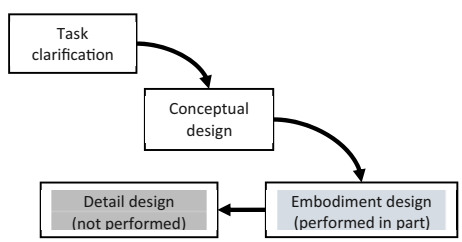

Note: In particular, the detail design phase is not considered for this preliminary investigation

and constrain the pressing element, the logical association was with platforms controlled by extending limbs and spherical joints.

However, for this particular application, only three degrees of freedom (dof) are needed, thus making useless the controls of the three rotational dof. A particular manipulator kinematics with three translational dof was proposed in 1996 (Tsai, 1996), which was also used for heavy structural applications, with an additional extensible limb (Boscaleri *et al.*, 2011). By taking inspiration from the latter, the proposed parallel manipulator has been conceived as shown in Figure 4. More specifically, the end effector (H) is connected to ground through four extendable legs. Two bodies internally connected with an actuated prismatic joint compose each jack. Legs are constrained to machine and end effector frames through cardan joints. For the kinematic analysis, cardan joints are treated as the assembly of two rotational joints with orthogonal axes.

To ease the understanding of the contents, a list of the used symbols is provided in Table 1.

As shown in Figure 4, both base frame and end effector are modelled as square shaped plates with side lengths, respectively, equal to $2p$ and $2r$. The system is over-constrained (a prismatic joint should be replaced with cylindrical ones), and over actuated (four actuators are used to control three dof). These unusual choices are justified by specifications concerning desired machine workspace, by potential advantages in terms of overall structural stiffness and finally by the possibility of exerting high vertical forces with a good accuracy exploiting all the four actuators working in parallel.

Figure 4 Simplified kinematic scheme of the proposed manipulator

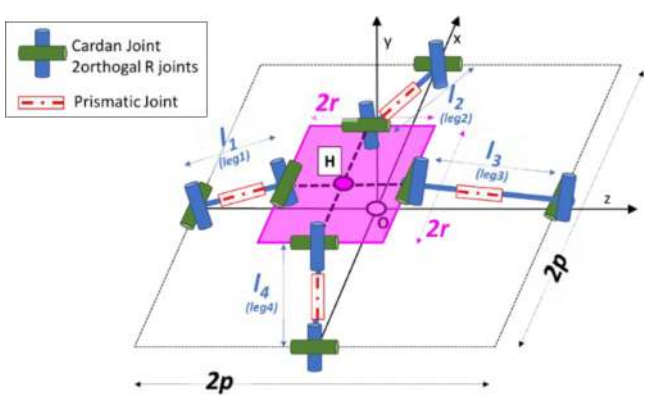

Table 1 List of symbols

Symbol	Description
H	Plate of the end effector
p	Half length of the square frame
r	Half length of the square plate of end effector
l_i	Length of the *i*th leg
x_h	*x* coordinate of the end effector
y_h	*y* coordinate of the end effector
z_h	*z* coordinate of the end effector
αi	Angle between the *i*th leg and the ground
βi	Angle between the *i*th leg and the neutral position

A known drawback of similar over-actuated manipulators (He *et al.*, 2006) is represented by non-zero internal forces that will occur if control inputs are incompatible. This feature imposes a high precision for what concern the control of actuators to avoid excessive internal structural loads. However, these internal loads if properly controlled should be useful to produce an optimal preload capable to reduce clearances of joints, improving precision and stiffness of the manipulator (Muller, 2005). This feature has consequences also for the choice of adopted actuators: direct drive actuators allowing a more precise four-quadrant control of exerted forces should be preferred for this kind of application and consequently for the proposed manipulator.

The kinematics is calculated by modelling each leg as an R-R-P serial manipulator (Figure 5), and then imposing additional conditions related to the closure of adopted kinematic chains. For the leg *i*th, three joints are considered, the two rotational joints of the cardan (rot. angle αi and βi), and a prismatic one able to modify the length li. The end effector H can only translate along the three axis x, y and z as proposed mechanism is substantially composed by two perpendicular four bar mechanisms which share the same kinematic member (plate H). Each of the two planar mechanisms allows a planar motion, respectively, in the planes yx and yz: as they share the plate H, thus not only rotations around y but also around x and z directions are not allowed.

The inverse-kinematic relations between the 12 joint variables corresponding to αi, βi, li and corresponding Cartesian coordinates of the end effector xh, yh and zh are described by equation (1).

As the system has two symmetry planes (yz and yx ones), the three relations that describe the kinematic behavior of one leg (as example the first one) can be reused to calculate also the kinematic of the other ones with trivial exchanges of variables that are also described in Table 2 and Figure 5:

Figure 5 Symbols adopted to describe kinematics of the *i*th leg

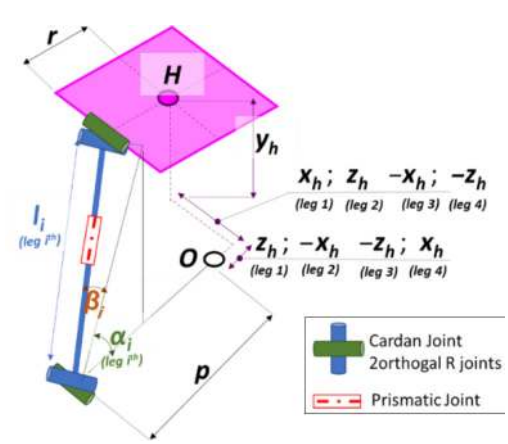

Table 2 Main symmetry props. of the proposed manipulator

Leg no.	Subs to be performed to reuse relations of leg 1 For leg *i*th
Leg 2	$x_h = z_h;\ z_h = -x_h;$
Leg 3	$x_h = -x_h;\ z_h = -z_h;$
Leg 4	$x_h = -z_h;\ z_h = x_h;$

$$\left.\begin{aligned}\alpha_1 &= \frac{y_h}{z_h + p - r};\\ \beta_1 &= \frac{x_h}{y_h}\sin\alpha_1;\\ l_1 &= \frac{y_h}{\cos\beta_1\sin\alpha_1};\end{aligned}\right\} leg\,1; \qquad \left.\begin{aligned}\alpha_2 &= \frac{-y_h}{x_h - p + r};\\ \beta_2 &= \frac{z_h}{y_h}\sin\alpha_2;\\ l_2 &= \frac{y_h}{\cos\beta_2\sin\alpha_2};\end{aligned}\right\} leg\,2;$$

$$\left.\begin{aligned}\alpha_3 &= \frac{-y_h}{z_h - p + r};\\ \beta_3 &= -\frac{x_h}{y_h}\sin\alpha_3;\\ l_3 &= \frac{y_h}{\cos\beta_3\sin\alpha_3};\end{aligned}\right\} leg3; \qquad \left.\begin{aligned}\alpha_4 &= \frac{y_h}{x_h + p - r};\\ \beta_4 &= \frac{z_h}{y_h}\sin\alpha_4;\\ l_4 &= \frac{y_h}{\cos\beta_4\sin\alpha_4};\end{aligned}\right\} leg\,4; \tag{1}$$

All over described calculations are performed in Matlab Simulink™ (Marghitu, 2009).

The derivatives of actuated leg lengths *li* respect to speed of the platform/end effector are described by equation (2):

$$\dot{l}_i = \frac{\dot{y}_h cos\beta_i \sin\alpha_i - y_i\left(-\dot{\beta}_i sin\beta_i \sin\alpha_i + \dot{\alpha}_i cos\beta_i \cos\alpha_i\right)}{\left(cos\beta_i \sin\alpha_i\right)^2} \tag{2}$$

Derivatives of angles αi and βi described in equation (2) are defined according to equation (3), where it is clearly visible that the symmetry properties can be also exploited to simplify the calculation of derivatives on different legs:

$$\begin{aligned}\dot{\alpha}_1 &= (\cos\alpha_1)^2\left(\frac{\dot{y}_h(z_h + p - r) - \dot{z}_h y_h}{(z_h + p - r)^2}\right)\\ \dot{\alpha}_2 &= (\cos\alpha_2)^2\left(\frac{-\dot{y}_h(x_h - p + r) + \dot{x}_h y_h}{(x_h - p + r)^2}\right)\\ \dot{\alpha}_3 &= (\cos\alpha_3)^2\left(\frac{-\dot{y}_h(z_h - p + r) + \dot{z}_h y_h}{(z_h - p + r)^2}\right)\\ \dot{\alpha}_4 &= (\cos\alpha_4)^2\frac{\dot{y}_h(x_h + p - r) - \dot{x}_h y_h}{(x_h + p - r)^2}\\ \dot{\beta}_1 &= (\cos\beta_1)^2\left(\dot{\alpha}_1\cos\alpha_1\frac{x_h}{y_h} + \left(\frac{\dot{x}_h y_h - x_h\dot{y}_h}{y_h}\right)\sin\alpha_1\right)\\ \dot{\beta}_2 &= (\cos\beta_2)^2\left(\dot{\alpha}_2\cos\alpha_2\frac{z_h}{y_h} + \left(\frac{\dot{z}_h y_h - z_h\dot{y}_h}{y_h}\right)\sin\alpha_2\right)\\ \dot{\beta}_3 &= -(\cos\beta_3)^2\left(\dot{\alpha}_3\cos\alpha\frac{x_h}{y_h} + \left(\frac{\dot{x}_h y_h - x_h\dot{y}_h}{y_h}\right)\sin\alpha_3\right)\\ \dot{\beta}_4 &= (\cos\beta_4)^2\left(\dot{\alpha}_4\cos\alpha_4\frac{z_h}{y_h} + \left(\frac{\dot{z}_h y_h - z_h\dot{y}_h}{y_h}\right)\sin\alpha_4\right)\end{aligned} \tag{3}$$

4. Preliminary embodiment evaluations

4.1 Kinematic evaluations

For a preliminary kinematic evaluation, it is considered a case study where it is supposed to have a workspace corresponding to a parallelepiped with a square base having a side of about 500 mm and an elevation of at least 100 mm. These specifications have been extracted by considering the datasheet of an existing machine (Fenix-Automation, 2021) as a reference. To meet these specifications, it is supposed to adopt a manipulator whose main geometric parameters are described in Table 3. Accordingly, the shape of the resulting workspace is visible in Figure 6. More specifically, the proposed manipulator complies with the design specifications in terms of workspace even considering imposed limitations on different joints. Figure 7 and 8 represent the behavior of derivatives of *l1* along significant *zx*, *zy* and *xy* planes for an assigned value of actuator elevation *yh*. The symmetry properties of the manipulator can be used to extend obtained results to other legs. The proposed solution appears to be well suited for the specific application, according to the desired specifications and prescribed workspace. Indeed, good margins respect to workspace limitations can be observed in Figure 6.

For what concerns the evaluation of manipulator dexterity, there is a wide literature (Boschetti and Trevisani, 2010; Merlet, 2005; Yoshikawa, 1985) concerning various indexes which are fundamentally based on the evaluation of the eigenvalues of the Jacobian matrix. As the proposed manipulator is over-actuated, the resulting Jacobian matrix is

Table 3 Main geometric dimensions of simulated manipulator

Parameter	VALUE
Minimum value l_{min} of length of a leg l_i	500 (mm)
Maximum value l_{max} of length of a leg *lmax*	1,000 (mm)
Maximum value α_{max} of the angle α_i	$\pi/2$ (rad)
Minimum value α_{min} of the angle α_i	0 (rad)
Maximum value β_{max} of the angle β_i	$\pi/4$ (rad)
Minimum value β_{min} of the angle β_i	$-\pi/4$ (rad)
Distance *p*	442 (mm)
Distance *r*	82 (mm)

Figure 6 Shape of the workspace respect to constraints imposed by different limitations on joints described in Table 3

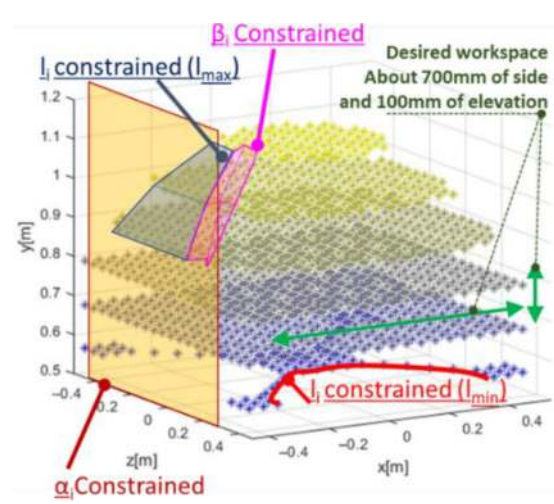

Figure 7 Joint derivatives vs speed of the end effector (*zx* plane with *yh* = 0.6 m)

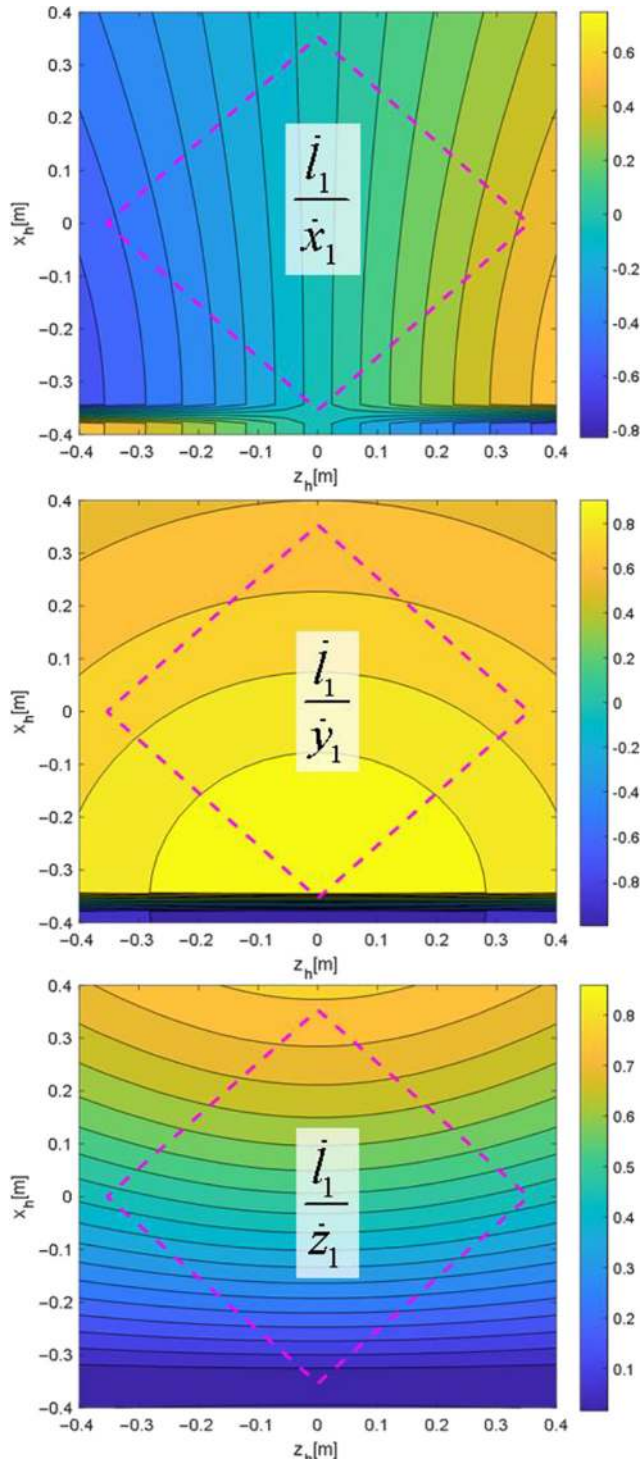

not square. Therefore, the dexterity of the index n [see equation (4)] is evaluated respect to maximum and minimum singular values (σmax, σmin) of the Jacobian matrix [which can be evaluated from equations (1)–(3)]:

$$n = \frac{\sigma_{\min}}{\sigma_{\max}} \tag{4}$$

In Figure 9, the values of n on a zx plane (y = 0.6 meters) within the chosen workspace are shown. In particular, iso-level curves of n are approximately rectangular; this is a useful feature considering the shape of desired workspace. However, the manipulator is far from being isotropic (n = 1), but the range of variability of n within workspace is limited (no more than 15%).

Specifications concerning maximum run and speed for actuators can be easily calculated from equations (1)–(3) that describe inverse kinematics of the manipulators. Solving static equilibrium between forces applied on end effector (X, Y and Z) and the four actuators (F1, F2, F3 and F4), it is possible to obtain the relation expressed by equation (5):

$$\begin{bmatrix} A_{11} & A_{12} & A_{13} & A_{14} \\ A_{21} & A_{22} & A_{23} & A_{24} \\ A_{31} & A_{32} & A_{33} & A_{34} \end{bmatrix} \begin{bmatrix} F_1 \\ F_2 \\ F_3 \\ F_4 \end{bmatrix} = \begin{bmatrix} X \\ Y \\ Z \end{bmatrix}$$

$$\begin{aligned} A_{11} &= \sin\beta_1; \\ A_{12} &= -\cos\beta_2 \cos\alpha_2; \\ A_{13} &= -\sin\beta_3; \\ A_{21} &= \cos\beta_1 \sin\alpha_1; \\ A_{22} &= \cos\beta_2 \sin\alpha_2; \\ A_{23} &= \cos\beta_3 \sin\alpha_3; \\ A_{24} &= \cos\beta_4 \sin\alpha_4; \\ A_{31} &= \cos\beta_1 \cos\alpha_1; \\ A_{32} &= \sin\beta_2; \\ A_{33} &= -\cos\beta_3 \cos\alpha_3; \\ A_{34} &= \sin\beta_4; \end{aligned} \tag{5}$$

It is possible to calculate a solution of system (5) by applying the pseudo-inversion approach of Moore–Penrose: obtained solution minimizes the norm 2 of forces on joints respect to forces exerted on hand effector. Indexes Fx (6), Fy (7) and Fz (8) are defined as the ratio between the infinite norm of joint forces (F1, F2, F3 and F4) and forces applied on the end effector respectively along x, y and z directions:

$$F_x = \frac{\|[abs(F_1.)..abs(F_4)]\|_\infty}{X} \tag{6}$$

$$F_y = \frac{\|[abs(F_1.)..abs(F_4)]\|_\infty}{Y} \tag{7}$$

$$F_z = \frac{\|[abs(F_1.)..abs(F_4)]\|_\infty}{Z} \tag{8}$$

The index Fy (Figure 10) is useful to determine the maximum value of the force required by the actuators respect to vertical loads on the end effector. It is interesting to notice that inside the workspace, this index is lower than one. Therefore, the forces exerted on joints are relatively small with respect to loads. Especially for configurations in which the end effector is aligned to the origin, the loads are almost equally shared between different actuators. The current selection of the workspace orientation respect to actuators is mainly optimized as visible in Figure 8, to maximize the condition number and consequently the isotropy of the manipulator. Results of

Figure 8 Joint derivatives (*zy* and *xy* planes)

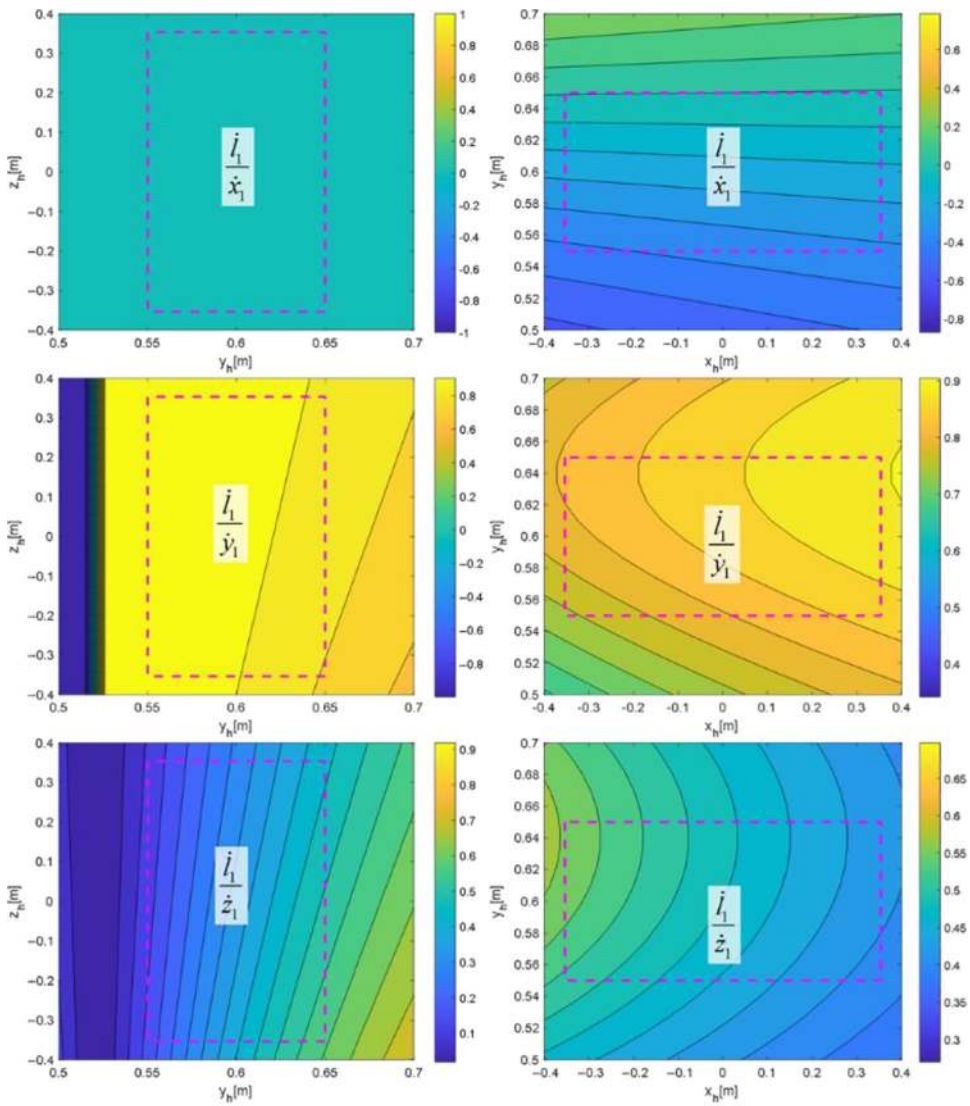

Note: Magenta dashed lines represent machine workspace according to specifications

Figure 9 Values of *n* on a *zx* plane (y_h = 0.6 m)

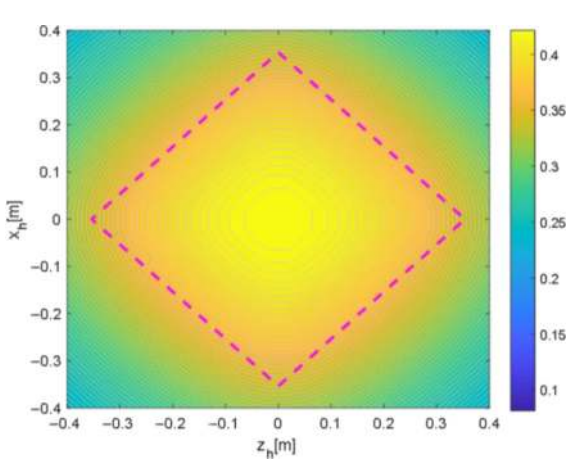

Figure 10 suggest that rotating the orientation of chosen workspace to 90 degrees, it is possible to considerably reduce forces on joints respect to desired vertical forces on end effector.

Figure 11 shows the behavior of *Fx*, while the behavior of *Fz* is not represented as because of symmetry properties of the manipulator, it can be easily predicted from *Fx*.

Indexes *Fx* and *Fz* are useful to understand the capability of the manipulator to exert forces on the *zx* plane, but their optimization is important to improve the dynamical performances of the actuator.

Finally, by performing a singular value decomposition of matrix A in equation (5), it is possible to map the behavior of four vectors $_v$ defined according to equation (9):

$$Av = \sigma u \tag{9}$$

Figure 10 Values of F_y respect to workspace

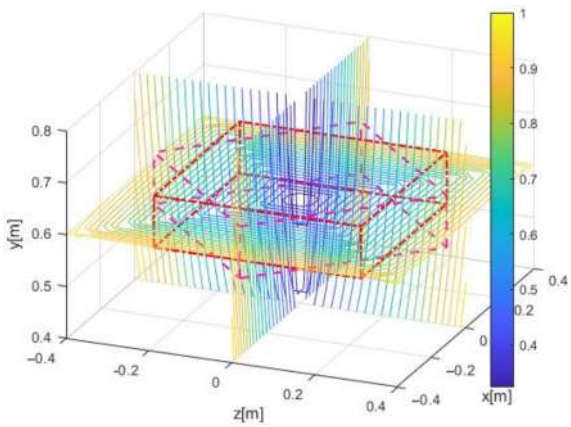

Note: Different orientations of limits workspace respect to manipulator are shown

Figure 11 Values of F_x respect to workspace

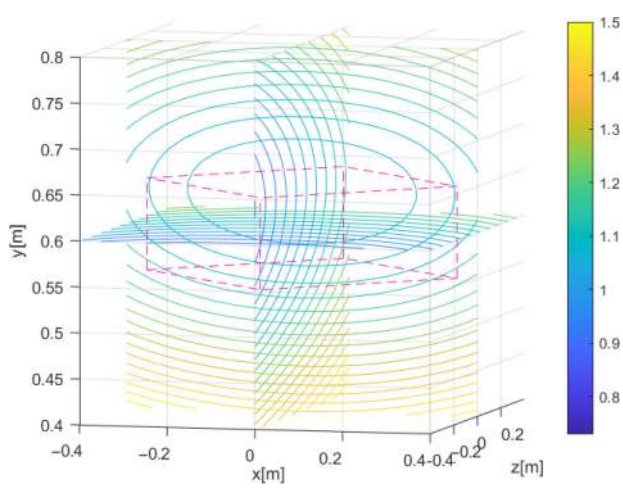

Vectors v are ordered in relation to the magnitude of the diagonal elements of σ. The first three vectors correspond to vectors of joint forces which produce corresponding variations of forces on X, Y and Z of the end effector. But the fourth one, which is defined here as v_p produce a null output on the end effector, causing exclusively an increase of internal preload of joints of the over-constrained structure of the manipulator. Some values of v_p respect to position of end effector are shown in Table 4.

Each vector of joint forces F_1, F_2, F_3 and F_4 can be decomposed in a linear combination respect to a base of four linearly independent vectors.

If the chosen base is represented by vectors v calculated according to singular value decomposition described in equation (9), weights a_i of the summatory (10) represent the four scalar coordinates which represent the vector of actuator forces F_i respect to this base:

$$F = \sum_{i=1}^{n} a_i v_i \tag{10}$$

Proposed structure has three dof and it is one time hyperstatic so the first three coordinates represent the three components of the vector of joint forces F which, respectively, produce a force on the hand effector respect to one of the three dof of the structure. The fourth one corresponds to the component which produces a null output increasing only structural preloads. This property can be exploited to calculate how forces on joints should produce an equivalent force on end effector, but also to recover clearances on joints by applying a proper preload which is substantially proportional respect to a4 the fourth coordinate respect to which is decomposed the vector of joint forces.

Calculation of v_p is fundamental for the future implementation of the direct control of desired preload on joints. These features currently not implemented should be useful to increase equivalent precision and stiffness of the manipulator by recovering clearances on joints.

4.2 Force control of the manipulator

Considering the proposed use of the manipulator (precise insertion of electronic components), both position and force controls must be implemented: position control is needed to properly control the trajectory of the manipulator, and once the component is properly positioned, a precise force limitation must be implemented for a proper insertion of the component on the board. Proposed control is described by the scheme in Figure 12 in this first simplified

Table 4 Tabulated values of v_p respect to a zx plane (y_h = 0.6 m)

x_h (m)	zh (m)					xh (m)	zh (m)				
			vp						vp		
0	0	−0.5	0.5	−0.5	0.5	0.35	0	−0.5	0.383	−0.5	0.594
0.1	0	−0.5	0.463	−0.5	0.535	−0.35	0	−0.5	0.594	−0.5	0.383
−0.1	0	−0.5	0.535	−0.5	0.463	0	0.35	−0.594	0.5	−0.383	0.5
0	0.1	−0.535	0.5	−0.463	0.5	0	−0.35	−0.383	0.5	−0.594	0.5
0	−0.1	−0.463	0.5	−0.535	0.5	0.35	0.35	−0.579	0.405	−0.405	0.579
0.1	0.1	−0.534	0.463	−0.463	0.534	−0.35	−0.35	−0.405	0.579	−0.579	0.405
−0.1	−0.1	−0.463	0.534	−0.534	0.463	0.35	−0.35	−0.579	0.579	−0.405	0.405
0.1	−0.1	−0.534	0.534	−0.463	0.463	−0.35	0.35	−0.405	0.405	−0.579	0.579
−0.1	0.1	−0.463	0.463	−0.534	0.534						

Figure 12 Simscape™ multibody model of the manipulator with proposed force limited position control

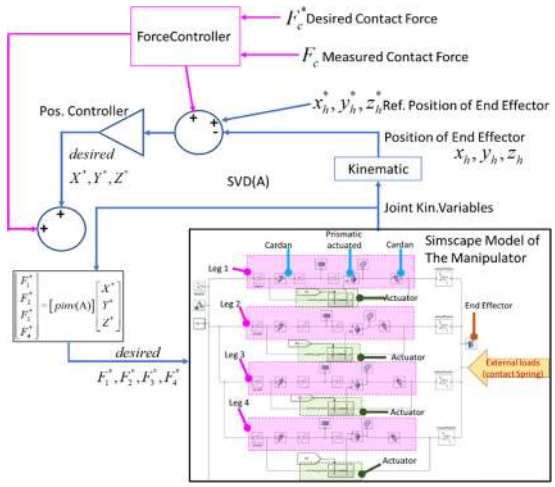

implementation: an external position control is implemented, desired position xh^*, yh^* and zh^* of the manipulator is compared with corresponding measured/estimated values that are calculated from the measurement of the run of the four linear actuators. Actuators are supposed to be directly force controlled; this assumption is needed to ensure a precise force control reducing the risk of potentially dangerous errors because of other disturbances such as nonlinear four quadrant behavior of actuators.

Limitations of insertion forces in the vertical direction are obtained according to the simplified scheme of Figure 12, where the contact force is measured to provide a proper feedback of a loop limiting the insertion forces, and modifying both the reference trajectory and the desired force reference delivered to actuators. Performances of this proposed control scheme should be further improved by introducing compensation of actuator weight and dynamics.

For what concerns proposed actuators, it is supposed to adopt a control bandwidth of exerted forces limited to 40 Hz, which is a feasible value as example for a servo-hydraulic systems (Pugi *et al.*, 2016, 2020). One of the main features of the proposed system is the adoption of a hyperstatic structure. This feature should be exploited to further increase stiffness and precision of the manipulator by controlling the application of limited preload on joints. This possibility is interesting but also involves a cautious choice and calibration of both actuators and control, especially in terms of equivalent mechanical impedance.

In Figure 13 and 14, an example of simulation is shown, starting from a known position of the end effector, which reaches the desired position of the component that have to insert, and then it moves vertically with an insertion force limited to 30 N and then return in a new position. Contact force is simply modelled considering an equivalent elastic element which produces a contact force that is proportional to the interference between the inserted component and the board.

4.3 Load distribution on legs

To perform a first evaluation of the loads distributed on the four legs, a computer-aided design (CAD) model has been

Figure 13 Example of simulated trajectory

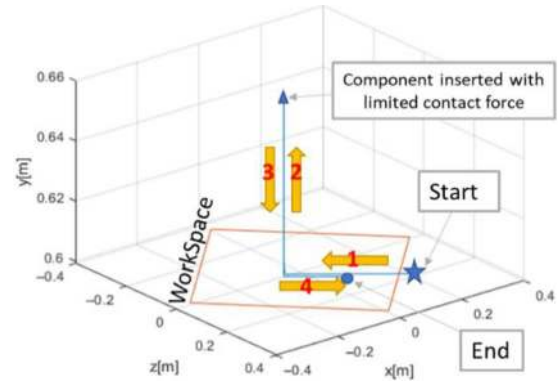

Figure 14 Contact force behavior during component insertion (it is considered a pure elastic contact), results with and without force limitation are shown

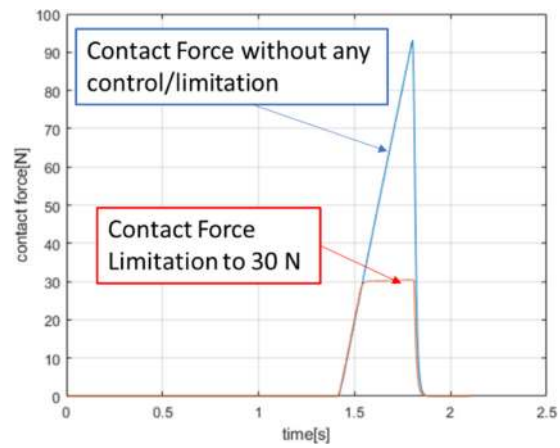

realized, according to the dimensions reported in Table 3. The considered geometry (Figure 15) should not be considered necessarily similar to the final aspect of the system, but is intended only to allow the simulation of the main kinematic elements.

Three different positions of the end effector have been considered (Figure 16) to evaluate the legs loads when the end effector is aligned with the origin, when it is within the base of two legs and when one of the legs is perfectly vertical. In particular, the second and the third conditions are assumed to be the potential worst conditions.

The static simulation has been performed with multibody models built on three different CAD models, one for each of the investigated configurations (Figure 16). In this case, it is important to put beforehand that as the considered geometry not represents a constructive embodiment, the stresses and deformations are not evaluated. Indeed, the structural behavior of the manipulator strongly depends on the particular solutions adopted to realize each critical part (i.e. legs, joints and plane).

Rotational joints with rigid behavior have been used to link the axes of each cardan joint. Differently, for each leg, the cylinder has been connected with a fixed joint to the respective stem, to simulate the effect a hypothetical actuator blocked in the desired position.

Figure 15 Reference CAD model of the manipulator used for the finite element method simulation

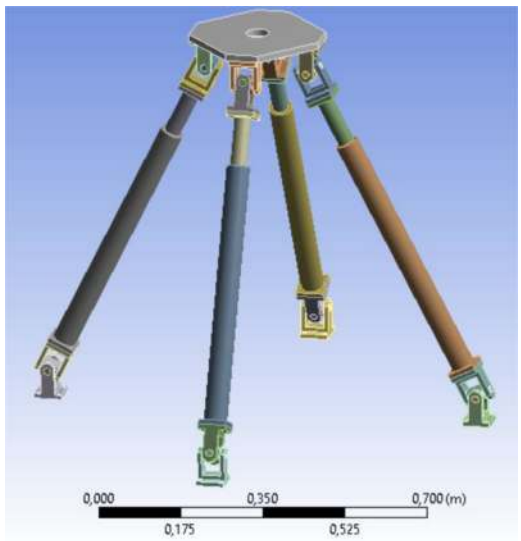

Figure 16 Geometrical configurations used to extract the load values on the four legs

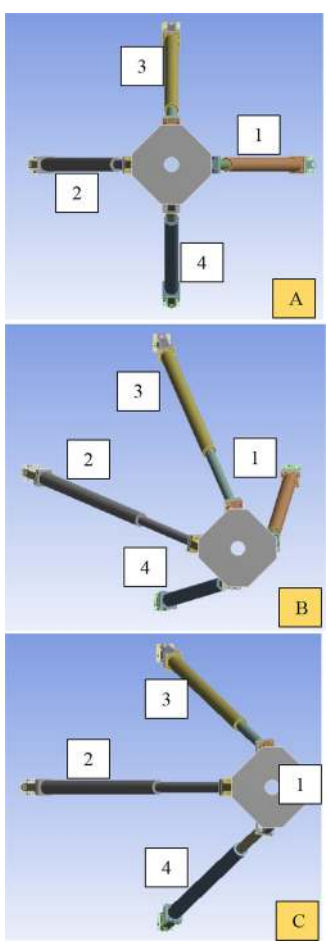

A preventive press load of 700 N has been considered, positioned in the middle of the upper plate and directed upward. The fixed joints have been used to extract the load values, by referring to the axis represented in Figure 17.

The load values extracted for each configuration of Figure 16 are reported in Tables 5 and 6, respectively, about forces and moments. Please note that possible unexpected asymmetries between values are because of the simulation. However, differences among symmetric elements are negligible.

The values reported in Tables 5 and 6 show that for design purposes, an axial load of about 500 N should be considered for the linear actuators used for each leg. However, the legs are also subjected to bending stresses, as shown in Table 6. It implies that the structural solution used to realize the extending legs and the related actuators should be designed with care, to avoid poor stiffness and/or buckling problems. Additionally, Table 6 also shows that when the end effector is far from being aligned with the origin, non-negligible torsional moments can affect the legs. Consequently, design choices should carefully consider that load, which could contribute to raise contact pressure on sliding elements.

Figure 17 Orientation of the three axes for each leg

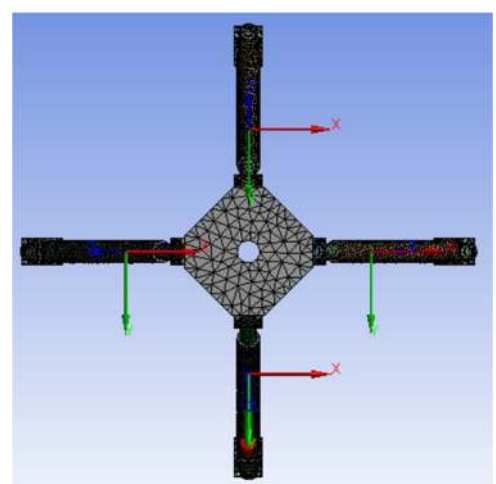

Table 5 Force components on legs

Case	Force components	Leg no. 1	2	3	4
Case A	*Fx* (N)	−3.6e-6	3.5e-6	1.3e-4	1.6e-4
	Fy (N)	−7.9e-5	-9.5e-5	3.6e-6	−3.6e-6
	Fz (N)	*−195.8*	*−195.8*	*−195.6*	*−195.6*
Case B	*Fx* (N)	1.8e-6	4.4e-6	4.3e-7	1.9e-6
	Fy (N)	1.6e-6	−9.9e-8	4.2e-7	1.5e-6
	Fz (N)	*−476.4*	*131.5*	*128.7*	*−479.1*
Case C	*Fx* (N)	3.6e-7	3.7e-6	1.7e-6	1.7e-6
	Fy (N)	1.4e-4	−7.7e-5	−8.9e-7	9.2e-7
	Fz (N)	*471.4*	*367.9*	*−299.8*	*−299.8*

Note: Noteworthy values are in italics

Table 6 Moment components on legs

Case	Moment components	Leg no. 1	2	3	4
Case A	*Mx* (Nm)	−3.7e-5	−1.0e-5	2.6e-8	−1.6e-8
	My (Nm)	1.8e-8	2.2e-8	−5.6e-5	−7.2e-5
	Mz (Nm)	9e-5	1.6e-4	−7.9e-5	−2.0e-4
Case B	*Mx* (Nm)	0.3	−0.5	*24.0*	*−6.0*
	My (Nm)	*6.1*	*−24.1*	*−2.6*	0.9
	Mz (Nm)	*16.0*	*−83.9*	*83.9*	*−17.1*
Case C	*Mx* (Nm)	1.3e-5	−9.1e-5	*38.3*	*−38.3*
	My (Nm)	−8.1e-9	4.3e-8	2.0e-6	2.0e-6
	Mz (Nm)	−9.9e-3	−2.7e-4	*82.2*	*−82.1*

Note: Noteworthy values are in italics

5. Discussions and conclusions

In this preliminary work, authors have presented a study concerning a redundant three-axis parallel manipulator which is based on an uncommon configuration with four actuated legs constrained by cardan and prismatic joints. The performed analysis is limited to a preliminary kinematic and static evaluation, fundamental to provide the information required for the succeeding phases of the design process. In particular, the correctness of the kinematics has been demonstrated, and an estimation of the loads acting on the legs has been performed. The method adopted to describe and solve joint kinematics of the proposed actuator is rather simplified in terms of implementation cost and more generally in terms of physically comprehension of the system even with a rudimentary knowledge of robotics. A force control system has been proposed and simulated. Models and indications are introduced, which are useful for the design of the actuation system to properly justify the adoption of direct drive actuators. At current state of the work, proposed solution seems to be feasible for the proposed application. Ongoing prosecution of this work is the design of a possible embodiment of proposed solution including a verification of possible interferences and a complete dynamic simulation of the system including control and actuation features. Once inertial and geometric properties of adopted components are completely known, also a more detailed modeling of actuation system including as example an electric or electro-hydraulic unit (Pulcinelli *et al.*, 2018).

This detailed model will be used also to obtain a preliminary foreseen of required power respect to realistic work cycles as proposed by Valigi *et al.* (2019).

It is also important to note that, to the authors' knowledge, this is the first paper that presents a comprehensive case study application of this kinematics. The data reported here provide important information and support the understanding of this particular solution, which could be conveniently reused for other applications, where parallel movements are needed (e.g. the printing heads of three-dimensional printers based on the fused deposition method).

References

Achilli, G.M., Valigi, M.C., Salvietti, G. and Malvezzi, M. (2020), "Design of soft grippers with modular actuated embedded constraints", *Robotics, Multidisciplinary Digital Publishing Institute*, Vol. 9 No. 4, p. 105.

Akay, D., Kulak, O. and Henson, B. (2011), "Conceptual design evaluation using interval type-2 fuzzy information axiom", *Computers in Industry*, Vol. 62 No. 2, pp. 138-146.

Beitz, W., Blass, E., Derhake, T., Derndinger, H.O., Ehrlenspiel, K., Franke, H.J., Gierse, F.J., *et al.* (1987), "VDI guideline 2221: Systematic approach to the design of technical systems and products (translation of the German edition 11/1986)", *VDI Guidelines*, VDI – Verlag, Düsseldorf, p. 1987.

Bernard, A., Coatanea, E., Christophe, F. and Laroche, F. (2014), "Design: a key stage of product lifecycle", *Procedia CIRP*, Vol. 21, pp. 3-9.

Boscaleri, A., Fiorineschi, L., Rissone, P., Baldi, M. and Zannoni, M. (2011), "A new approach in designing of stratospheric platforms aimed at multi-user LDB flights", *European Space Agency*, (Special Publication) ESA SP, Vol. 700 SP.

Boschetti, G. and Trevisani, A. (2010), "Direction selective performance indexes for parallel manipulators", *The1st Joint International Conference on Multibody System Dynamics*.

Botello-Aceves, S., Valdez, S.I., Becerra, H.M. and Hernandez, E. (2018), "Evaluating concurrent design approaches for a delta parallel manipulator", *Robotica*", , Vol. 36 No. 5.

Chen, P. (2008), "U.S. Patent No. 7,377,823."

Fenix-Automation (2021), "Datasheet of PTH components assembly cell AO-00", available at: line at the site of Fenix Automation www.fenixautomation.com"

Gosselin, C.M., Masouleh, M.T., Duchaine, V., Richard, P., Foucault, S. and Kong, X. (2007), "Parallel mechanisms of the multipteron family: kinematic architectures and benchmarking", *Proceedings 2007 IEEE International Conference on Robotics and Automation*, pp. 555-560.

Haidegger, T., Galambos, P. and Rudas, I.J. (2019), "Robotics 4.0 – are we there yet?", *2019 IEEE 23rd International Conference on Intelligent Engineering Systems (INES)*, pp. 117-124.

He, G., Tan, X.-L., Zhang, X.-H. and Lu, Z. (2006), "Optimal synthesis of a planar 3-DOF overactuated full-compliant parallel mechanism", *Chinese Journal of Mechanical Engineering*, Vol. 20 No. 3.

Le Masson, P. and Weil, B. (2012), "Design theories as languages of the unknown: insights from the German roots of systematic design (1840–1960)", *Research in Engineering Design*, Vol. 24 No. 2, pp. 105-126.

Marghitu, D.B. (2009), *Mechanisms and Robots Analysis with MATLAB®*, Springer Verlag, London.

Merlet, J.P. (2005), "Jacobian, manipulability, condition number, and accuracy of parallel robots", *Journal of Mechanical Design*, Vol. 128 No. 1, pp. 199-206.

Muller, A. (2005), "Internal preload control of redundantly actuated parallel manipulators – its application to backlash avoiding control", *IEEE Transactions on Robotics*, Vol. 21 No. 4, pp. 668-677.

Pahl, G., Beitz, W., Feldhusen, J. and Grote, K.H. (2007), *Engineering Design 3rd Ed*, Springer-Verlag London, doi: 10.1007/978-1-84628-319-2.

Peruzzi, A., Pugi, L. and Berzi, L. (2021), "Design optimization of a Cartesian assembly cell", *Mechanisms and Machine Science*.

Pugi, L., Alfatti, F., Berzi, L., Favilli, T., Pierini, M., Forrier, B., D., T., *et al.* (2020), "Fast modelling and identification of hydraulic brake plants for automotive applications", *International Journal of Fluid Power*, Vol. 21 No. 2, pp. 169-210.

Pugi, L., Galardi, E., Pallini, G., Paolucci, L. and Lucchesi, N. (2016), "Design and testing of a pulley and cable actuator for large ball valves", *Proceedings of the Institution of Mechanical Engineers, Part I: Journal of Systems and Control Engineering*, Vol. 230 No. 7, pp. 622-639.

Pulcinelli, A., Pugi, L., Vinattieri, F., Capitani, R. and Annicchiarico, C. (2018), "Design and testing of an innovative electro-hydraulic actuator for a semi-active differential", *Proceedings of the Institution of Mechanical Engineers, Part D: Journal of Automobile Engineering*, Vol. 232 No. 11, pp. 1438-1453.

Tsai, L.W. (1996), "Kinematics of a Three-Dof platform with three extensible limbs", in: LenarCic, J. and Parenti-Castelli, V. (Eds), *Recent Advances in Robot Kinematics*, Kluwer Academic Publishers, pp. 401-410.

Valigi, M.C., Logozzo, S., Landi, L., Braccesi, C. and Galletti, L. (2019), "Twin-Shaft mixers' mechanical behavior numerical simulations of the mix and phases", *Machines, Multidisciplinary Digital Publishing Institute*, Vol. 7 No. 2, p. 39.

Wynn, D.C. and Clarkson, P.J. (2017), "Process models in design and development", *Research in Engineering Design*, Springer London, No. July, pp. 1-42.

Yoshikawa, T. (1985), "Manipulability of robotic mechanisms", *The International Journal of Robotics Research*, Vol. 4 No. 2, pp. 3-9.

Corresponding author

Lorenzo Fiorineschi can be contacted at: lorenzo.fiorineschi@unifi.it

For instructions on how to order reprints of this article, please visit our website:
www.emeraldgrouppublishing.com/licensing/reprints.htm
Or contact us for further details: **permissions@emeraldinsight.com**